Collisional quenching and *j*-mixing rate constants for the 3*D* levels of Ca^+

Martina Knoop, Michel Vedel, and Fernande Vedel*
Physique des Interactions Ioniques et Moléculaires, UMR 6633 CNRS-UAM1, Centre de St. Jérôme, Case C21, F-13397, Marseille Cedex 20, France

(Received 22 October 1997; revised manuscript received 12 December 1997)

Collisional relaxation and fine-structure mixing rate constants have been measured for the metastable *D* doublet ($3D_{3/2}$, $3D_{5/2}$) of Ca^+ ions in the presence of different neutral gases completing a previous work. Experimental results are given for He, Ne, Ar, H_2, N_2, and CH_4. These data have been obtained with a cloud of approximately 10^5 Ca^+ ions stored in a Paul trap at kinetic energies of around 1 eV. The investigated levels were populated by direct excitation of the corresponding $4S$-$3D$ transitions. The involved time constants were determined from the temporal evolution of the fluorescence of one of the resonance transitions, following the optical pumping of the *P* level from the *D* component. Comparison of our data with other similar experimental and theoretical work is finally presented. [S1050-2947(98)03807-4]

PACS number(s): 32.80.Pj, 32.50.+d, 07.75.+h

I. INTRODUCTION

The technique of ion storage is unique to prepare and observe ions for long times under very well-controlled pressure conditions and without interactions with the walls [1]. These properties allow one to imagine frequency standards, the performances of which are comparable to or better by some orders of magnitude than the existing standards [2]. Demonstration of this fact has already been made in the microwave region [3], and various propositions exist in the optical domain. Additionally, ion storage offers the possibility to observe the temporal evolution of ion species (prepared eventually in selected internal states) under various effects. This property can be used to study the influence of neutral gases on the lifetime of atomic levels, especially metastable states. Thus collisional reaction rates are accessible even for very long-lived levels. Such types of data are indeed required to evaluate the influence of the unavoidable collisions on the limits of accuracy for frequency standards based on stored ions. Actually, the quantum jump statistics involved in the long term stabilization is modified by the collisions still occurring at ultrahigh-vacuum conditions ($p<10^{-9}-10^{-10}$ mbar). On the other hand, quantitative values of pressure line broadening are needed for the interpretation of astrophysics observations and to model the dynamics of interstellar clouds.

The Ca^+ ion is a very attractive candidate for an optical frequency standard at 410 THz. The weak electric quadrupole transition ($4S_{1/2}-3D_{5/2}$) at 729 nm (Fig. 1) leads to a high quality factor of 2×10^{15}. The existence of an odd nuclear spin ($I=\frac{7}{2}$ for $^{43}Ca^+$) gives rise to transitions independent of weak magnetic field ($m_F=0\rightarrow m_{F'}=0$), minimizing residual effects. One of the pertinent advantages of this ion is the fact that the transitions needed for the laser cooling and the probing of the clock transition can be generated by diode lasers, either directly or by frequency doubling. Due to their small natural linewidths, the Ca^+ forbidden lines are also used as calibration lines in astrophysics.

The metastable $3D$ doublet has been studied before, theoretically as well as experimentally [4]. The related lifetimes have been measured either with a large cloud at quasithermal energies [5–7], with a small laser-cooled ion cloud [8], or with the technique of quantum jumps [9,10]. We have carried out a systematic investigation of the influence of collisions on the $3D$ levels of Ca^+. In this paper, we present results which complete our previous measurements. Quenching and *j*-mixing rates will be given for the noble gases helium, neon, argon, and for the molecular gases hydrogen, nitrogen, and methane. All the data were obtained by direct population of the investigated levels, a method which avoids parasitic population in the neighboring states [7].

II. EXPERIMENT

The experiments reported here were carried out in a device previously described [7] (Fig. 2). A cloud of approximately 10^5 Ca^+ ions is stored in a medium-sized traditional Paul trap ($r_0=7.2$ mm). Its endcaps are made from molybdenum mesh with high transmission (85%) in order to be able to observe a maximum of fluorescence emitted by the stored ion cloud. The trap is working under UHV conditions (residual pressure below 7×10^{-10} mbar) which are maintained by a 100*l* ion pump, a turbomolecular pump being used for the initial evacuation. Trapping parameters are V_{ac}

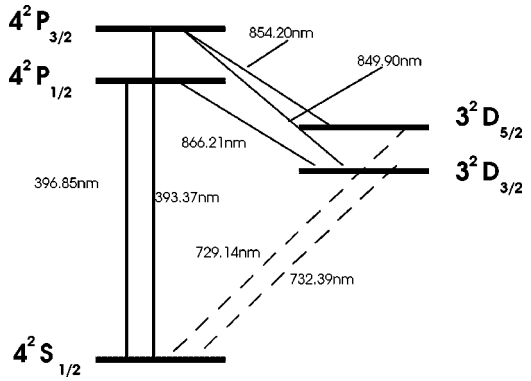

FIG. 1. First energy levels of $^{40}Ca^+$.

*Electronic address: FERN@FRMRS12.U-3MRS.FR

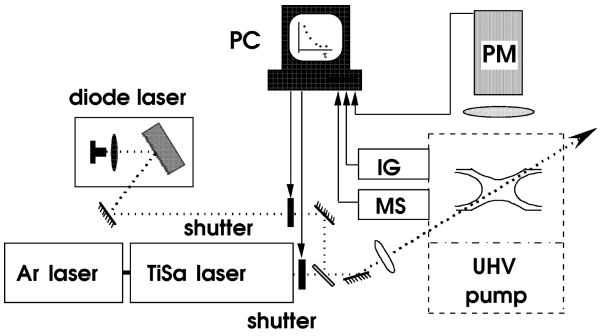

FIG. 2. Experimental setup. IG: ion gauge; PM: photomultiplier; MS: mass spectrometer λ; TiSa: titane-sapphire..

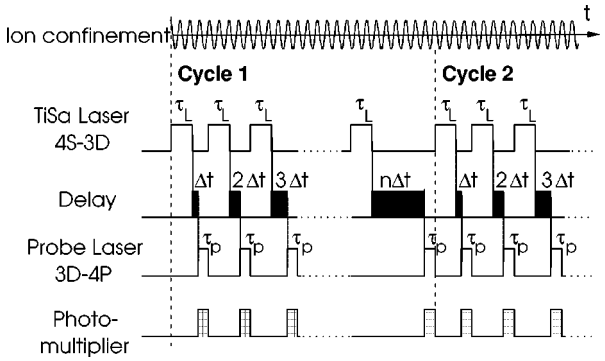

FIG. 3. Time sequence of the laser application during the quenching experiment.

$=530V_{\mathrm{eff}}$, $\Omega/2\pi=2.18$ MHz, $V_{\mathrm{dc}}=0$V, corresponding to $q_z=0.74$, and $a_z=0$. These values have been carefully chosen to optimize the size and the temperature of the ion cloud and to avoid ion loss or ion heating due to nonlinear resonances [11]. The applied voltage creates a total pseudopotential well of approximately 100 eV ($D_r=34.5$ eV, $D_z=66.5$ eV). This relatively deep potential assures an efficient confinement of the ion cloud even in the presence of a heavy buffer gas like argon.

Neutral gases are introduced through a leak valve. This permits impurity-free introduction of the buffer gas in a range of 10^{-9}–10^{-5} mbar. The gas composition is measured by a quadrupole mass spectrometer (Balzers QMG 064) with a resolution better than 1×10^{-9} mbar. The total pressure is monitored by a Bayard-Alpert ion gauge (Granville-Phillips 330 IG). Both devices have to be turned off during measurement because of the fluorescence of their cathodes, and due to their strong electron emission which causes residual ion creation. The pressure values can be read and stored automatically with the personal computer unit controlling the experiment. The upper limit of the partial pressure range is determined by the performance of the ion pump ($p\leqslant10^{-5}$ mbar). The lower pressure is limited by the shortness of the ion confinement duration and by the delicate stability of the gas composition during the experiment. The smallest partial pressures used are around 4×10^{-9} mbar.

The 729- and 732-nm radiations, needed to excite the $4S_{1/2}$–$3D_{5/2}$ and $4S_{1/2}$–$3D_{3/2}$ transitions, are given by the fundamental wave of a cw Ti-Sa laser (Coherent 899-21), pumped with a 10-W argon-ion laser with a maximum power of 1 W. The 854- and 866-nm transitions are generated by single-mode diode lasers (Institut Poljus, SDL) placed into external cavities which allows fine tuning of the wavelength. The output powers of the diode lasers are lower than 1 mW, that is largely sufficient for the optical pumping of the ions out of the metastable state. All the laser beams cross the trap diagonally. They are precisely overlapped and focused into the center of the ion cloud.

To access the quenching rate, we operate as following (Fig. 3). After introducing one neutral gas species at a given pressure, one of the electric quadrupole transitions ($4S_{1/2}$–$3D_{3/2}$, $4S_{1/2}$–$3D_{5/2}$) is excited during 1000 ms, a duration long enough to transfer the complete ionic population to the metastable state. Then, after a variable delay, the populated level $3D_{3/2}$ ($3D_{5/2}$) is probed with the corresponding laser $3D_{3/2}$–$4P_{1/2}$ ($3D_{5/2}$–$4P_{3/2}$). Saturation of the $3D$-$4P$ transition allows one to consider that all the ions are pumped to the P state. The intensity of the fluorescence on the resonance line ($4P$-$4S$) is then directly proportional to the ion number in the $3D$ level. The fluorescence signal is measured by a photomultiplier running in the photon-counting mode. Varying the delay will visualize the exponential decay of the considered $3D$ level for a given set of partial pressures. For the mixing rate measurements, a similar experimental protocol is applied, with the difference that probing of the $3D_{3/2}$ level corresponds to initial populating of the $3D_{5/2}$ state, and vice versa. Additionally, the $3D$-$4P$ probe laser is switched on during the population time τ_L, to assure that the investigated level is initially unoccupied. For a good signal-to-noise ratio of the decay curve, measurement cycles are repeated 20–40 times in both cases (Fig. 4). Pressure measurements are carried out before and after each accumulation cycle. The experiment is interrupted every ten accumulation cycles to proceed to an automatic partial pressure measurement.

Varying the pressure in the trap will also change the kinetic energy of the ion cloud. As the ratio of elastic to inelastic collisions is different for each gas species, their respective influences on the ion temperature are not identical. The temperature of the ion cloud is checked from the reso-

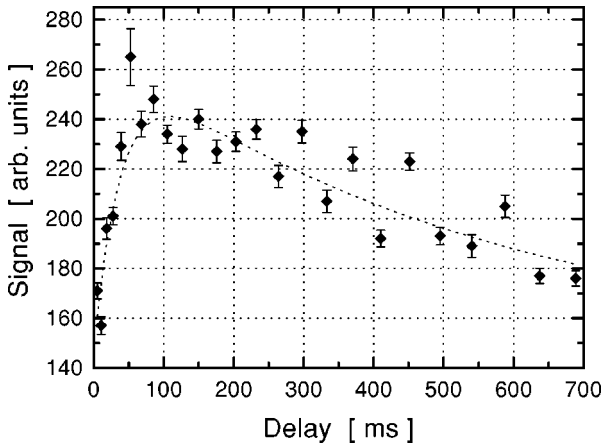

FIG. 4. Temporal evolution of the fine structure mixing process from the $3D_{5/2}$ to $3D_{3/2}$ level at a neon partial pressure of $p_{\mathrm{Ne}}=9\times10^{-7}$ mbar. Here the $3D_{3/2}$ level is initially empty; it fills rapidly because of mixing with the $3D_{5/2}$ state. For longer delay times, deexcitation to the ground state due to the finite lifetime and to quenching collisions becomes predominant.

nance Doppler profile recorded for every partial pressure set. Overall minima (0.6 eV) and maxima (1.6 eV) values are close enough together that here we may consider the rate constant to be roughly independent of temperature. Before each run we also look at the ion loss, which generally has a time constant of a couple of hours, but can be quite important for heavy gases. Care is taken to carry out measurements only at pressures for which the ion-loss time constant is greater than 2 min. Simulation of the quenching (or j-mixing) decay including this ion loss then shows that the maximum error due to the superimposition of two time constants is 20%. In our experiment, this phenomenon is without importance for all gases but argon. Argon has the same atomic mass as calcium, and it tends to kick the ions out of the trap. Accumulation cycles for this gas were reduced to ~10, leading to a rather high statistical error.

III. RESULTS AND DISCUSSION

Quenching measurements were carried out 134 times for the $3D_{3/2}$ level, and 149 times for $3D_{5/2}$. As the energy difference between the metastable states is negligible (7.4 meV) compared to the energy difference between the metastable doublet and the ground state (1.7 eV), we may suppose that the quenching rates Γ_Q for both states of the doublet are identical. Every single measurement yields a measured time constant τ_Q, the value of which depends on a set of partial pressures:

$$\frac{1}{\tau_Q} = \frac{1}{\tau_{\text{nat}}} + \sum_i n_B^i \Gamma_Q^i, \tag{1}$$

where i stands for each gas present in the UHV vessel: H_2, He, CH_4, Ne, N_2, O_2, Ar, and CO_2. Water vapor pressure was also monitored during each run; these partial pressures were, however, negligible. Even though H_2, O_2, and CO_2 were not actively introduced, their pressure contribution could be measured, as small quantities were either desorbed from the pump or from the vessel or created by dissociation. The latter is true especially for the introduction of methane, which gave rise to a nonnegligible pressure of hydrogen. Nevertheless, overall O_2 and CO_2 partial pressures were not sufficient to allow a correct quantitative evaluation of their influence on the quenching.

In Fig. 5, the measured inverse lifetimes have been represented as a function of the total buffer gas density. The points have been labeled according to the gas which has been introduced into the UHV vessel. This gas then has the highest partial pressure. Nevertheless, due to the abovementioned dissociation and desorption processes, other gases can reach rather important partial pressures. The ratio between the different partial pressures depends on the absolute value of the buffer gas density, and cannot be regarded as being constant. As a consequence, the alignment of points in Fig. 5 does not necessarily follow a simple straight-line fit.

To take into account the varying composition of the total buffer gas and the respective influences of the different components, the determined quenching and j-mixing time constants were fitted by a multilinear fit using a least-squares method [12]. Details of the fitting method as well as the analytical expression of the ion dynamics necessary for the

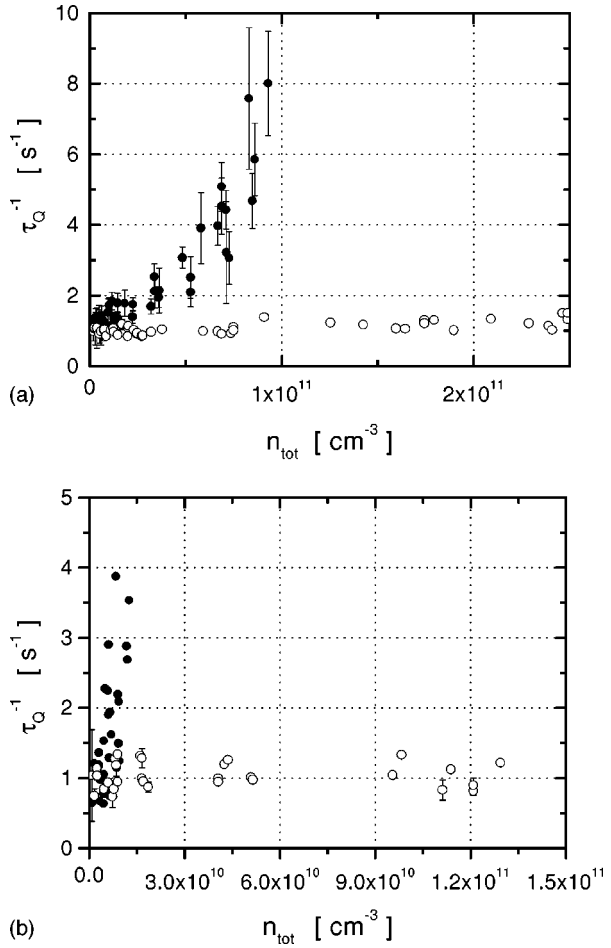

FIG. 5. Stern-Volmer plot for the quenching values. The inverse lifetimes are represented as a function of the total pressure (sum of the partial pressures). This representation does not exhibit the different influences of the various gas compositions. All ordinate error bars are purely statistical. For reasons of readability, the error bars for the Ar values have not been plotted in this graph. The average error bar values are given in parentheses. (a) ○: He (6%); ●: CH_4 (19%); (b) ○: Ne (7%); ●: Ar (75%).

determination of the respective quenching and j-mixing time constants were given in Ref. [7]. From the experimental data, it was possible to extract the collisional quenching, and j-mixing, rate values for H_2, He, CH_4, Ne, N_2, and Ar. The error of each absolute pressure measurement was estimated to be of the order of 30%. Various gases are measured with different precisions, and each set of partial pressures is composed in a different way. Nevertheless, the mass spectrometer is assumed to be linear in the considered pressure range. The large number of data sets can improve the precision on the final results.

Table I, where the quenching rates for He, Ne, and N_2 presented in Ref. [7] are also indicated, clearly shows the strong quenching influence of molecular buffer gases compared to helium and neon. Among the atomic buffer gases, argon seems to play a different role, which is most probably due to its higher mass. The molecular buffer gases show growing quenching rates as a function of their atomic mass, since the proportion of inelastic collisions becomes more important. The evolution of the quenching rate coefficients as a function of polarizability α shows increasing values indepen-

TABLE I. Quenching rate constants for the $3D$ levels of Ca^+.

Gas	m (amu)	α (10^{-24} cm^3)	Γ_Q (10^{-12} cm^3 s^{-1})	k_L (10^{-10} cm^3 s^{-1})	k_L/Γ_Q
H_2	2	0.804	37 ± 14	15.2	41 ± 15.5
He	4	0.205	1.05 ± 0.40	5.56	529 ± 201
CH_4	16	2.593	54^{+91}_{-17}	11.15	$21^{+35}_{-6.5}$
Ne	20	0.396	0.9 ± 0.7	4.03	448 ± 348
N_2	28	1.74	170 ± 20	7.61	4.5 ± 0.5
Ar	40	1.64	29.5 ± 17.0	6.70	23 ± 13

dent of the type of the collision partner.

There are few works about quenching rate constants of ions with neutral gases. Measurements involving metastable levels of trapped ions are given in Table II. In this table, values for Pb^+, N^+, and Ar^{2+} have been included for comparison, as they have been measured using the same buffer gases and working at similar collision energies, even though their electronic level scheme is quite different from those of the alkaline-earth ions Ca^+, Ba^+, and Yb^+. For a more complete review of quenching experiments, in particular for different collision energies, see Ref. [20].

With the exception of the work of Madej and Sankey [14], which has been made by observing the quantum jump statistics of a single, laser-cooled Ba^+ ion, the presented experiments have been carried out on hot ion clouds at temperatures of several thousand K. All measurements confirm the greater efficiency of molecular gases for inelastic quenching collisions. This fact is due to the existence of a large number of rotational and vibrational degrees of freedom in the quenching gas. As a consequence, internal energy can easily be transferred in a wide range. The experiment on a single Ba^+-ion results in values superior to all other measurements with alkaline-earth ions. This is most probably due to the experimental conditions, since higher quenching rates are expected at lower temperatures [21,22].

Measurements of the fine-structure mixing have been made for the $3D_{3/2}$ to $3D_{5/2}$ (149 values) as well as for the inverse process ($3D_{5/2}$ to $3D_{3/2}$, 166 values). Curves obtained as in Fig. 4 allow one to determine the time-constants for the mixing process at a given pressure. The fine-structure mixing rates γ_{53} (for the j-mixing of $3D_{5/2}$ toward $3D_{3/2}$) and γ_{35} (for the j-mixing of $3D_{3/2}$ toward $3D_{5/2}$) are defined by

$$\frac{1}{\tau_{\text{meas}}}=\sum_i n_B^i \gamma_{jj'}^i . \tag{2}$$

The values as given by the multilinear fit are listed in Table III.

j-mixing measurements have been carried out in a smaller pressure range (approximately 1.5 decades per gas) as the signal is difficult to detect. In fact, if the pressure is too high, the j-mixing process is very fast, and the temporal evolution of the ion population can no longer be resolved. For very low pressures, mixing becomes weaker, and the fluorescence signal becomes very small. Since all the gases have different cross sections, this pressure range varies for each gas. The considered intervals lie between 1×10^{-8} and 5×10^{-6} mbar.

Here again, a rate constant for hydrogen could be determined. Unfortunately, it was only possible to extract the γ_{53} for H_2 with a reasonable precision. The ratio of γ_{35} to γ_{53} can be evaluated from the principle of detailed balancing, and should be equal to $\frac{3}{2}$, for our physical conditions. Given the large error bars due to the pressure measurements, the obtained ratios are in fairly good agreement with the theory.

Other measurements of fine-structure mixing of metastable states of Ca^+ [9,23,24] exist. All these experiments concern mixing from the $3D_{3/2}$ to the $3D_{5/2}$ level under the influence of hydrogen. The values are given to be 5×10^{-10}, 7×10^{-10}, and $(1.97\pm0.16)\times10^{-9}$ cm^3/s, respectively. Although they have been obtained for different collision energies, their values are nevertheless quite close to our experimental results.

One can compare the measured values to the classical Langevin reaction rate constants k_L. From Fig. 6, it is evi-

TABLE II. Quenching rate constants for the metastable states of different stored ions. ΔE stands for the energy difference which separates the studied level from the ground state. All measured rate constant values are given in 10^{-12} cm^3 s^{-1}.

Ion	State	ΔE	H_2	He	CH_4	Ne	N_2	Ar	Ref.
Ba^+	$5D_{3/2,5/2}$	0.7 eV	37 ± 3	0.3 ± 0.02		0.51 ± 0.04	44 ± 3		[13]
Ba^+	$5D_{5/2}$	0.7 eV	350 ± 50	10 ± 3	600 ± 80		230 ± 30	7 ± 5	[14]
Ca^+	$3D_{3/2,5/2}$	1.7 eV	37 ± 14	1.05 ± 0.40	54^{+91}_{-17}	0.9 ± 0.7	170 ± 20	29.5 ± 17.0	this work
Yb^+	$5D_{3/2}$	2.85 eV	10.2 ± 1				178 ± 19		[15]
Yb^+	$5D_{3/2}$	2.85 eV					155 ± 41		[16]
Pb^+	$6P_{3/2}$	1.75 eV	$\leqslant25\pm12.5$	$\leqslant1.2\pm0.6$			$\leqslant8.2\pm4.1$		[17]
Ar^{2+}	3^1S_0	3.95 eV						550 ± 80	[18]
N^+	2^5S_2	5.8 eV					2500^{+2500}_{-1250}		[19]

TABLE III. Fine-structure mixing rates for the metastable $3D$ levels of Ca^+.

Gas	γ_{35} (10^{-10} cm^3 s^{-1})	γ_{53} (10^{-10} cm^3 s^{-1})	γ_{35}/γ_{53}
H_2		3 ± 2.2	
He	2.24 ± 0.10	1.2 ± 0.5	1.9 ± 0.9
CH_4	34 ± 14	41 ± 12	0.85 ± 0.6
Ne	5.5 ± 2.2	1.3 ± 0.6	4.2 ± 3.7
N_2	28 ± 3	12.6 ± 1.0	2.2 ± 0.45
Ar	7.7 ± 3.4	2.7 ± 1.1	2.85 ± 2.4

dent that quenching and j-mixing rates present a similar behavior as a function of k_L. Species with a lower Langevin rate constant show small quenching and j-mixing values. The ratio of measured reaction rate constants to k_L passes by a maximum around $k_L \approx 1\times10^{-9}$ cm^3/s before it slightly falls off towards higher Langevin rates. j-mixing rates are always found to be significantly higher than quenching rates, in some cases up to two orders of magnitude [Fig. 6(a)]. This can be roughly explained by the Landau-Zener model taking into account the energy of the studied transition [7]. For comparison, we introduced the values of another ion trap experiment [14] into this graph [Fig. 6(b)]. Even though the data are quite different due to a much lower temperature and a different collision partner (Ba^+, $m=138$ amu), the shape of the plotted curve fits well our results.

There have been two theoretical approaches to the fine-structure mixing rate of Ca^+ with helium. Both are fully quantal close-coupling calculations. In Ref. [25], the variation of γ_{53} with temperature was determined to be $\gamma_{53} = 0.456(T/1000\ K)^{0.23}\times10^{-9}$ cm^3/s with an uncertainty of 5%. At a temperature of 10 000 K, this is equivalent to $\gamma_{53}=(7.7\pm0.4)\times10^{-10}$ cm^3/s. In a more recent paper [22], the j-mixing process was studied and the relative collisional cross sections were determined for kinetic energies up to 2.5 eV. The rate constants at 10 000 K are found to be $\gamma_{35} = 12.33\times10^{-10}$ cm^3/s and $\gamma_{53}=8.29\times10^{-10}$ cm^3/s. Both calculations are in quite good agreement, even though the values put forward are more than a factor of 5 higher than our experimental results. A comparable high ratio between calculated and measured data has been found for the mixing of the Ca^+ $4P$ states [26]. At temperatures below 5000 K, theoretical values were calculated to be 3–5 times higher than experimental values.

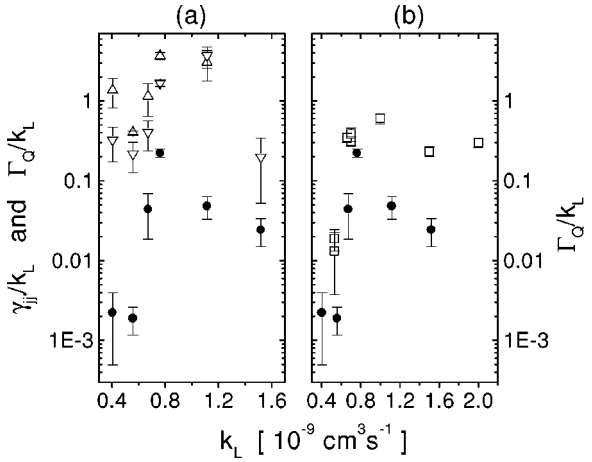

FIG. 6. (a) Ratios of the quenching (●) and j-mixing (△,▽) rates to the Langevin reaction rates k_L, as a function of k_L for various collision partners. (b) Ratios of the quenching rates to the Langevin reaction rates k_L, as a function of k_L, from this work (●) and from Ref. [14] (□).

These disagreements between calculations and experiments reflect the difficulties in the theoretical approach of the collisional relaxation process. The dominant mechanism for the mixing of the fine-structure levels appears to be the breakdown of spin-orbit and, at larger distances, Coriolis coupling due to the electrostatic and magnetic interactions [27,26]. Insight into the mechanism of the quenching process, where the separation of the involved energy levels is superior to 1 eV, can only be gained by careful examination of the interaction potentials of the pseudomolecule which is formed by the colliding partners during the collision process. Nonadiabatic coupling mechanisms determine the importance of the deexcitation process due to inelastic collisions. In general, atomic selection rules cannot be applied systematically in the evaluation of the strength of interaction [28,7]; they are not valid in the case of collisions with molecular gases [27].

IV. CONCLUSION

We have presented a systematic experimental investigation of the influence of different neutral buffer gas species on the metastable $3D$ levels of Ca^+. Quenching and fine-structure mixing rate constants for three atomic and three molecular buffer gases have been measured. Comparison with other experiments shows a good general agreement. The values obtained by close-coupling calculations are significantly higher than the measured rate constants. This is not only true for the Ca^+ $3D$ levels but has also been found for the mixing of the $4P$ levels [26] as well as for the pressure broadening of the $4P$-$3D$ triplet [25].

Very few experimental works exist for this type of data, in spite of a strong request for astrophysical as well as metrological applications. More experimental results would be helpful for a better understanding of the collisional processes and for the further improvement of the theoretical models. Further data are still necessary at lower energies in order to be able to totally control the collisional influence of residual gases on a single, laser-cooled ion. We plan now to measure the collisional processes at low temperatures with a single ion in a miniature trap by observation of the quantum jumps statistics. As the kinetic energy of the center-of-mass changes only by a factor of 3 for an ion with a temperature around 100 mK, the anticipated values are supposed to lie slightly higher than the values we measured throughout this work.

ACKNOWLEDGMENTS

Our experiment was supported by the Bureau National de Métrologie, Direction des Recherches et Etudes Techniques, and Conseil Général des Bouches du Rhône.

[1] W. Paul, Rev. Mod. Phys. **62**, 531 (1990).
[2] *Proceedings of the Fifth Symposium on Frequency Standards and Metrology*, edited by J. C. Bergquist (World Scientific, Singapore, 1996), and references therein.
[3] R. L. Tjoelker, J. D. Prestage, and L. Maleki, in *Proceedings of the Fifth Symposium on Frequency Standards and Metrology* (Ref. [2]), p. 33–38.
[4] E. Biemont and C. J. Zeippen, Comments At. Mol. Phys. **33**, 29 (1996).
[5] F. Arbes, T. Gudjons, F. Kurth, G. Werth, F. Marin, and M. Inguscio, Z. Phys. D **25**, 295 (1993).
[6] F. Arbes, M. Benzing, T. Gudjons, F. Kurth, and G. Werth, Z. Phys. D **29**, 159 (1994).
[7] M. Knoop, M. Vedel, and F. Vedel, Phys. Rev. A **52**, 3763 (1995). Note that the D_i variables in Eqs. (7) and (8) should read $D_1=2[\Gamma_{\rm nat}+n_B\Gamma_Q]$ and $D_2=2[\Gamma_{\rm nat}+n_B(\Gamma_Q+\gamma_{35}+\gamma_{53})]$. This correction does not modify the given results.
[8] T. Gudjons, B. Hilbert, P. Seibert, and G. Werth, Europhys. Lett. **33**, 595 (1996).
[9] S. Urabe, K. Hayasaka, M. Watanabe, H. Imajo, and R. Ohmukai, Jpn. J. Appl. Phys. **33**, 1590 (1994).
[10] G. Ritter and U. Eichmann, J. Phys. B **30**, L141 (1997).
[11] R. Alheit, S. Kleineidam, F. Vedel, M. Vedel, and G. Werth, Int. J. Mass Spectrom. Ion Processes **154**, 155 (1996).
[12] MINUIT, CERN Program Library Entry D506, CERN, Genève 1992.
[13] A. Hermanni and G. Werth, Z. Phys. D **11**, 301 (1989).
[14] A. A. Madej and J. D. Sankey, Phys. Rev. A **41**, 2621 (1990).
[15] C. Gerz, J. Roths, F. Vedel, and G. Werth, Z. Phys. D **8**, 235 (1988).
[16] D. J. Seidel and L. Maleki, Phys. Rev. A **51**, R2699 (1995).
[17] A. Roth, Ch. Gerz, D. Wilsdorf, and G. Werth, Z. Phys. D **11**, 283 (1989).
[18] M. H. Prior, Phys. Rev. A **30**, 3051 (1984).
[19] R. D. Knight, Phys. Rev. Lett. **48**, 792 (1982).
[20] D. A. Church, Phys. Rep. **228**, 253 (1993).
[21] R. Zhang and D. R. Crosley, J. Chem. Phys. **102**, 7418 (1995).
[22] E. Paul-Kwiek and E. Czuchaj, Z. Phys. D **41**, 87 (1997).
[23] S. Urabe, K. Hayasaka, M. Watanabe, H. Imajo, R. Ohmukai, and R. Hayayashi, Appl. Phys. B **57**, 367 (1993).
[24] M. Benzing, Diplomarbeit, Johannes-Gutenberg-University, Mainz/FRG, 1994 (unpublished).
[25] T. S. Monteiro, I. L. Cooper, A. S. Dickinson, and E. L. Lewis, J. Phys. B **20**, 741 (1987).
[26] J. Brust, M. Movre, and K. Niemax, Z. Phys. D **27**, 243 (1993).
[27] E. E. Nikitin, *Theory of Elementary Atomic and Molecular Processes in Gases* (Clarendon, Oxford, 1974).
[28] E. W. McDaniel, J. B. A. Mitchell, and M. E. Rudd, *Atomic Collisions—Heavy Particle Projectiles* (Wiley, New York, 1993).